Review article: Necessity of Direct Dose Measurement during Current X-ray Diagnosis -Our Approach Using a Small-type OSL Dosimeter-

Authors:

[1,*] Hiroaki Hayashi, PhD
[1)]Yoshiki Mihara
[1)] Yuki Kanazawa, PhD
[1)] Emi Tomita
[1)] Sota Goto
[2)] Kazuki Takegami
[3)] Tohru Okazaki
[3,4)] Takuya Hashizume
[3)] Vergil Lorenzo Estacio Cruz

Authors note :

1) Graduate School of Health Sciences, Tokushima University, Japan
2) Department of Radiological Technology, Yamaguchi University Hospital, Japan
3) Nagase Landauer, Ltd., Japan
4) SOKENDAI, Japan

***Corresponding Author**

770-8503 Kuramoto 3-18-15, Tokushima, Japan

E-mail: hayashi.hiroaki@tokushima-u.ac.jp

Abstract:

During current medical X-ray diagnosis, an automatic exposure control system is widely used. The system can provide proper X-ray exposure, which varies by the patients' physical type. It is difficult to measure exposure dose using a traditional dosimeter. Therefore, it is proposed that it is possible to use a small-type OSL dosimeter for direct dose measurements. For this application, evaluation of basic properties such as angular and energy dependences is important. Moreover, even when derived, some ideas are needed to apply this information to dosimetry. In this paper, the concept of a calibration curve using 83 kV X-rays is introduced and it is proposed that an uncertainty of 15% should be added. Moreover, when dosimeter is applied to CT examination, consideration of pitch factor is needed. It is estimated that the uncertainty of PF is at most 25%, and overall uncertainty will be approximately 30%. It is also important to determine whether or not the dosimeter influences the medical image. Typical X-ray images of chest X-ray and CT scan of whole body are presented, and an explanation that the OSL dosimeter can be applied to actual clinical examinations.

Keywords:

OSL dosimeter; direct dose measurement; diagnostic X-ray; CT examination;

1. Introduction

In current medical examinations, X-rays have been widely used, and there is a lot of research concerning proper management of exposure doses [1, 2]. The advantage of using X-rays for these examinations is to achieve short examination time and high-resolution medical images. Recently, a new technique, called an automatic exposure control (AEC) system, can make it possible to reduce exposure dose [3-6]; using this technique, the amount of irradiated X-rays are automatically determined so as to obtain proper medical images. However, from the view point of management of exposure dose, the current situation is very complexed. Appropriately it is thought that a new approach to managing exposure dose is needed.

Figure 1 shows a comparison between three different situations of general X-ray examinations in which entrance-skin dose (ESD) should be managed. (a) shows an actual situation, the ESD is results from the exposure of incident X-rays and back-scattering X-rays. However, the ESD to the actual patient is difficult to measure because many available dosimeters interfere with medical images; therefore many phantom studies have been carried out [7]. Section (b) shows a general method using an air-kerma measurement. In theory, air-kerma of incident X-rays is measured by an ionization chamber, and the contribution of back-scattering X-rays is corrected. The correction is known as back-scatter-factor (BSF) and many reports are published on this topic [8-11]. This estimation method is widely used, but there are demerits; the method does not take into consideration the effect of complexed structures, such as human bodies, and also cannot be applied to diagnosis in which exposure dose is automatically determined by AEC. Based on the above considerations, a new management method using a small-type optically stimulated luminescence (OSL) dosimeter has been proposed. Using a dosimeter, direct dose measurement can be carried out as shown by section (c) in Fig. 1.

In this paper, the characteristics of the small-type OSL dosimeter for dose management in actual X-ray diagnosis are reviewed.

2. General properties of a small-type OSL dosimeter

2.1. Construction

The small-type OSL dosimeter, named nanoDot, is commercially available by Landauer, Inc. There are many reports concerning nanoDot OSL dosimeters [12-27], and most of the reports are concerned with the radiation therapy region [12,16,17,20]. It is important to study the basic characteristics of the nanoDot OSL dosimeters in the diagnostic energy region [11-14].

Initially a description the construction of the dosimeter will be presented. This information is useful when carrying out a Monte-Carlo simulation. For many researchers, it is difficult to obtain a schematic drawing of the detector. Fortunately, Lehmann et al. published detailed construction data (cross sectional view of the detector) using a micro-CT (see Fig. 5 in reference [17]). Based on this published data, one can easily see it's simplified construction of the nanoDot OSL dosimeter. One example used in our simulation is illustrated in Fig. 2. Detection material is composed of Al_2O_3: C and glue (polyester), and the outer region (plastic case) is made of acrylonitrile-butadiene-styrene (ABS) resin. Table 1 summarizes a detailed description of the detection region. As shown in this table, three different compositions are reported. Kerns et al. [16] and Lehmann et al. [17] used the data to simulate the response of the nanoDot OSL dosimeter using a megavoltage photon beam and they compared with experimental results; although the data for high energy X-rays are in good agreement with the simulated data, it is unclear that these reports can be applied to the diagnostic X-ray region. Jursinic [18] reviewed the above mentioned research and used the data and an estimation to verify this experimental data.

Recently, there have been difficulties in the simulation have been noticed [28]. In the simulation, it is important to construct the actual detection components, which may be compositions of Al_2O_3 and polyester, but in an actual situation, we can measure the luminescent light from Al_2O_3. In the current Monte-Carlo simulation, it is difficult to reproduce a situation in which powder type Al_2O_3 is found in polyester, and only the energy absorption of the Al_2O_3 powder can be calculated. This problem still remains. In this paper, presents the results in which the detection region consists of 100% Al_2O_3 with thickness 0.2 mm and effective density 1.41 g/cm^3.

2.2. Dosimetry for clinical situations using the nanoDot OSL dosimeter

Here, clinical situations which measure exposure doses are assumed. Figure 3 shows a schematic drawing of a chest X-ray. Generally speaking, air-kerma of direct X-rays should be measured, because the air-kerma is strongly related to the management of amount of X-ray exposure, and if need, the ESD can be assumed as described above. Using nanoDot OSL dosimeters, to the measurement of not only air-kerma of direct X-ray but also ESD and air-kerma of scattered X-rays is proposed. To achieve these goals, the responses of the nanoDot OSL dosimeter, such as angular dependence and energy dependence, should be evaluated. This point is completely different from that of general dosimetry. During the air-kerma measurement of direct X-ray, the research scientist should check the quality of X-ray as a parameter of half-value layer of aluminum [29], and the there is no need to evaluate angular dependence. On the other hand, when researchers want to evaluate air-kerma of scattered X-rays and ESD, which are caused by direct X-ray and scattered X-rays (containing different angles and energies), the angular and energy dependence should be estimated. Moreover, when one plans to measure ESD in an actual clinical situation, the research scientist should check whether the dosimeter interferes with the medical image or not. If these problems are solved properly, dosimetry using a nanoDot OSL dosimeter will become an important topic in the radiology; only direct measurements can evaluate the actual dose under the AEC technique.

Figure 4 shows another example, in which nanoDot OSL dosimeter is used during computed tomography (CT) [25]. Section (a) shows a demonstration of the phantom study, in which approximately 100 dosimeters are set on the surface of the human body phantom. Then, whole-body scans were performed without and with AEC, and the resulting dose distributions are presented in (b) and (c), respectively. A significant dose reduction in the chest region can be observed, however there is not a large difference in the abdomen region. As just described, the AEC technique plays an important role in current X-ray diagnosis, and a new dose evaluation procedure is hoped for.

2.3. Angular dependence

Because the nanoDot OSL dosimeter has a disk geometry, there is an angular dependence. There are few reports concerning the angular dependence in the diagnostic X-ray region [13], therefore our precise data are valuable. [19, 23]. Typical results for angular dependence against 40 kV X-rays are presented in Figure 5 (a). The blue open circles show experimental data, which are measured using pure X-ray beams; namely, an original collimator [30] to reduce scattering X-rays generated from the movable diaphragm [31] was used. The red dashed line shows simulated results; which was performed using Monte-Carlo simulation code EGS5 [32]. The simulated data are in good agreement with the experiment. A rapid drop in responses at 0.7 at 90 degrees and 270 degrees can be seen; in these situations, nanoDot OSL dosimeters were irradiated from a side direction, which was caused by geometrical restrictions. When the research scientist uses a nanoDot OSL dosimeter during a general X-ray examination, the scientist pays attention to the direction of the nanoDot OSL dosimeter; when the nanoDot OSL dosimeters are necessarily set at the positions where X-rays will be incident from side directions, the scientist should correct for the difference of efficiency (angular dependence). The precise data for angular dependence are found in references [19, 23].

Moreover a more useful simulation, in which X-rays were randomly irradiated to the nanoDot OSL dosimeter was carried out. Figure 5 (b) shows the results. The horizontal axis is tube voltage of X-rays. The results clearly indicate that the change of efficiency is at most -4% when compared with zero degree. This result strongly supports the validity of direct exposure dose measurement, when the nanoDot OSL dosimeters are used to measure scattering X-rays and/or X-rays during CT examinations.

2.4. Energy dependence

In addition to the angular dependence, the energy dependence is important, because both the energy and angle of Compton scattered X-rays differ from the incident X-rays [33].

The energy dependence of the nanoDot OSL dosimeter is represented in Figure 6. The blue open circles show measured data by Gasparian et al. [22]; they carried out measurements using a standard X-ray field. Energy dependence was measured using characteristic X-rays [21] and results were consistent with Gasparian's data. The red dashed line shows simulated results using EGS5 code. The simulated data is in good agreement with the experiments. In the diagnostic energy range, the response of the nanoDot OSL dosimeter rapidly changed. The response rises to the 3.5 level at 30 keV, and it falls right down to the 1.0 level at 100 keV, and it is steady at 1.0 to a higher energy region. When scientists use the nanoDot OSL dosimeter in the diagnostic region, the scientist should pay attention to the differences in response.

3. A unique method to evaluate exposure dose in the diagnostic X-ray region

3.1. Calibration curve

As represented above, the nanoDot OSL dosimeter has a relatively small angular dependence and a relatively large energy dependence in the diagnostic energy region. Therefore, when the scientist wants to evaluate exposure doses at each measurable point as described in Fig. 3 and/or Fig. 4, they should consider the effect properly.

In order to consider these effects, a unique method [24] is being proposed. In a previous paper, Takegami et al. proposed a way to add proper uncertainty; namely, it was determined that a calibration curve having a proper uncertainty could be available instead of precise corrections for angular and energy dependencies. A calibration curve with 83 kV X-rays was constructed, and it was verified that the curve can be used for both air-kerma and ESD measurements when an additional 15% of uncertainty is applied to the measured value. The results of the calibration curve are represented by Figure 7. The red dashed line shows the calibration curve, which was made from air-kerma of 83 kV X-rays, as shown in the upper graph of Fig. 7. Then it was determined that the air-kerma of different tube voltages (55 kV and 108 kV) and ESDs concerning different X-ray fields (diameters of 10 cm, 20 cm, and 30 cm) are consistent with the calibration curve, and the differences of these data from the calibration curve are within the 15% uncertainty as shown in the lower graph of Fig. 7. A previous paper [24] reports that the origin of this 15% uncertainty could be analyzed by error propagation of the following elements: 5% was from the individualities of the dosimeters (systematic uncertainty), 5% from angular dependence, 10% from energy dependence, and so on. Note that the energy dependence should be evaluated by the effective energies of continuous X-ray spectra used during diagnosis. The detailed analysis is described in reference [24]. In this way, the effect of energy and angular dependencies when determining the uncertainties of the calibration curve was taken into consideration, therefore the analysis of exposure doses without irradiation condition information can be achieved.

When scientists want to use dosimeters during CT examinations, the consideration of pitch factors (PF) is needed. When PF equals 1.0, dosimeters attached on the patients will be irradiated uniformly. But this is rare during clinical examinations, and a normal examination does not use a PF of 1.0 and an over beaming effect should be considered. Therefore, some dosimeters will be irradiated by both direct and scattered X-rays, and others will be irradiated by only scattered X-rays. In order to consider the difference, the effect of PF on exposure doses was examined, and it was concluded that scientists should add an additional 25% uncertainty when the nanoDot OSL dosimeter is applied to CT examinations having a PF of less than 1.0 [25]. Coupled with the consideration of angular and energy dependences (15% uncertainty), it was determined that the exposure dose can be estimated to be approximately 30%.

This knowledge strongly helps the direct measurement of exposure doses in clinical situations. Recently research scientists measured exposure dose during actual clinical examinations using the nanoDot OSL dosimeter [26, 27] and the present data supports those results.

3.2. Capability for medical application

For applying the dosimeter to the medical X-ray examination, influence on the medical images should be discussed in addition to the scientific evidence described in the above section.

In Figure 8, two typical examinations using phantoms are presented. Figure 8 (a) and (b) show experimental arrangements of the chest X-ray diagnosis and CT examination, respectively. The nanoDot OSL dosimeters are placed on the surface of the phantoms. Section (c) shows the X-ray image taken using a computed radiography system [34,35]. In this image, the nanoDot OSL dosimeters cannot be clearly identified; this fact means that the dosimeter did not interfere with the X-ray image during a typical X-ray examination. This laboratory has published other evidence concerning the invisibility using spectrum measurement, and in the previous paper the limitations of the use of the nanoDot OSL dosimeter [36] have been discussed. The use of the nanoDot OSL dosimeter during general X-ray examinations is suspected especially in the irradiation field; therefore, if scientists want to apply these kinds of dosimetry, it is recommended that they confirm the lack of detection for the equipment used. On the other hand, the nanoDot OSL dosimeter can be identified in the CT image [25], but there are no harmful artifacts; therefore, it is thought that the nanoDot OSL dosimeter can provide valuable information concerning exposure dose during CT examination.

4. Conclusion

In this paper, the characteristics of the nanoDot OSL dosimeter have been reviewed with the aim that it is used for the direct exposure dose measurement in clinical situations. Current typical X-ray examinations and CT examinations use a technique called AEC, and the exposure dose may vary for each patient. It is thought that the nanoDot OSL dosimeter can be applied to direct dose measurements under consideration of angular and energy dependences. In previous studies carried out by this laboratory, it was verified that the uncertainties will be 15% for general X-rays and 30% for CT examinations. In the future it is hoped that the procedure of direct measurements of exposure doses can lead more safe medical tests, and provide valuable information for both patients and medical staff.

5. References

[1] González A.B, Darby S., Risk of cancer from diagnostic X-rays: estimates for the UK and 14 other countries, The Lancet 363, 345-351(2004). Doi: 10.1016/S0140-6736(04)15433-0

[2] Uffmann M., Schaefer-Prokop C., Digital radiography: The balance between image quality and required radiation dose, European Journal of Radiology 72, 202-208(2009). Doi: 10.1016/j.ejrad.2009.05.060

[3] Use of an Automatic Exposure Control Mechanism for Dose Optimization in Multi-Detector Row CT Examinations: Clinical Evaluation, Radiology 237, 213-223(2005). Doi: 10.1148/radiol.2363041220

[4] Kalra M.K., Rizzo S.M.R., Noveline R.A., Reducing radiation dose in emergency computed tomography with automatic exposure control techniques, Emergency Radiology 11, 267-274(2005). Doi: 10.1007/s10140-004-0395-7

[5] Pascoal A., Lawinski C.P., Maxkenzie A., et al., Chest radiography: a comparison of image quality and effective dose using four digital systems, Radiation Protection Dosimetry 114, 273-277(2005). Doi: 10.1093/rpd/nch572

[6] Veldkamp W.J., Kroft L.J., Boot M.V., et al., Contrast-detail evaluation and dose assessment of eight digital chest radiography systems in clinical practice, European Radiology 16, 333-341(2006). Doi: 10.1007/s00330-005-2887-6

[7] Matsunaga U., Kawauchi A., Kobayashi K., et al., Dose Estimation for Exposure Conditions of Diagnostic Radiology Acquired by a 2011 Questionnaire in a Phantom Study, Japanese Journal of Radiological Technology 69, 1372-1378(2013). Doi: 10.6009/jjrt.2013_JSRT_69.12.1372

[8] Klevenhagen S.C., Experimentally determined backscatter factors for x-rays generated at voltages between 16 and 140 kV, Physics in Medicine and Biology 34, 1871-1882(1989). Doi: 10.1088/0031-9155/34/12/010

[9] Grosswendt B., Backscatter factors for x-rays generated at voltages between 10 and 100 kV, Physics in Medicine and Biology 29, 579-591(1984). Doi: 10.1088/0031-9155/29/5/010

[10] Grosswendt B., Dependence of the photon backscatter factor for water on source-to-phantom distance and irradiation field size. Physics in Medicine and Biology 35, 1233-1245(1990). Doi: 10.1088/0031-9155/35/9/004

[11] Kato H., Method of calculating the backscatter factor for diagnostic X-rays using the differential backscatter factor,

Japanese Journal of Radiological Technology 57, 1503-1510(2001).

[12] Jursinic P.A., Characterization of optically stimulated luminescent dosimeters, OSLDs, for clinical dosimetric measurements, Medical Physics 34, 4594-4604(2007). Doi: 10.1118/1.2804555

[13] Al-Senan R.M., Hatab M.R., Characteristics of an OSLD in the diagnostic energy range, Medical Physics 38, 4396-4405(2011). Doi: 10.1118/1.3602456

[14] Hayashi H., Nakagawa K., Okino H., et al., High accuracy measurements by consecutive readings of OSL dosimeter, Medical Imaging and Information Science 31, 28-34(2014). Doi: 10.11318/mii.31.28

[15] Nakagawa K., Hayashi H., Okino H., et al., Fabrication of Annealing Equipment for Optically Stimulated Luminescence (OSL) Dosimeter, Japanese Journal of Radiological Technology 70, 1135-1142(2014). Doi: 10.6009/jjrt.2014_JSRT_70.10.1135

[16] Kerns J.R., Kry S.F., Sahoo N., et al., Angular dependence of the nanoDot OSL dosimeter, Medical Physics 38, 3955-3962(2011). Doi: 10.1118/1.3596533

[17] Lehmann J., Dunn L., Lye J.E., et al., Angular dependence of the response of the nanoDot OSLD system for measurements at depth in clinical megavoltage beams, Medical Physics 41, 061712-1-9(2014). Doi: 10.1118/1.4875698

[18] Jursinic P.A., Angular dependence of dose sensitivity of nanoDot optically stimulated luminescent dosimeters in different radiation geometries, Medical Physics 42, 5633-5641(2015). Doi: 10.1118/1.4929558

[19] Hayashi H., Takegami K., Okino H., et al., Procedure to measure angular dependences of personal dosimeters by means of diagnostic X-ray equipment, Medical Imaging and Information Science 32, 8-14(2015). Doi: 10.11318/mii.32.8

[20] Reft C.S., The energy dependence and dose response of a commercial optically stimulated luminescent detector for kilovoltage photon, megavoltage photon, and electron, proton, and carbon beams, Medical Physics 36, 1690-1699(2009). Doi: 10.1118/1.3097283

[21] Takegami K., Hayashi H., Okino H., et al., Energy dependence measurement of small-type optically stimulated luminescence (OSL) dosimeter by means of characteristic X-rays induced with general diagnostic X-ray equipment, Radiological Physics and Technology 9, 99-108(2016). Doi: 10.1007/s12194-015-0339-9

[22] Gasparian P.B.R., Vanhavere F., Yukihara E.G., Evaluating the influence of

experimental conditions on the photon energy response of Al_2O_3:C optically stimulated luminescence detectors, Radiation Measurements 47, 243-249(2012). Doi: 10.1016/j.radmeas.2012.01.012

[23] Okazaki T., Hayashi H., Takegami K., et al., Fundamental Study of nanoDot OSL Dosimeters for Entrance Skin Dose Measurement in Diagnostic X-ray Examinations, Journal of Radiation Protection and Research 41, 229-236(2016). Doi: 10.14407/jrpr.2016.41.3.229

[24] Takegami K., Hayashi H., Okino H., et al., Practical calibration curve of small-type optically stimulated luminescence (OSL) dosimeter for evaluation of entrance skin dose in the diagnostic X-ray region, Radiological Physics and Technology 8, 286-294(2015). Doi: 10.1007/s12194-015-0318-1

[25] Takegami K., Hayashi H., Yamada K., et al., Entrance surface dose measurements using a small OSL dosimeter with a computed tomography scanner having 320 rows of detectors, Radiological Physics and Technology, in press. Doi: 10.1007/s12194-016-0366-1

[26] Tappouni R., Mathers B., Scan Quality and Entrance Skin Dose in Thoracic CT: A Comparison between Bismuth Breast Shield and Posteriorly Centered Partial CT Scans, ISRN Radiology 2013, 457396-1-6(2013). Doi: 10.5402/2013/457396

[27] Chetlen A.L., Brown K.L., King S.H., et al., Scatter Radiation Dose From Digital Screening Mammography Measured in a Representative Patient Population, American Journal of Roentgenology 206, 359-365(2016). Doi: 10.2214/AJR.15.14921

[28] Okazaki T., Hayashi H., Okino H., et al., Calculation of energy and angular dependences of the small-type OSL dosimeter in the diagnostic and nuclear medicine regions using the Monte-Carlo simulation code, International Conference on Medical Physics (ICMP2016), Thailand, Dec. 9-12 (2016).

[29] Ariga E., Ito S. Deji S. et al., Determination of half value layers of X-ray equipment using computed ragiography imaging plates, Physica Medica 28, 71-75(2012). Doi: 10.1016/j.ejmp.2011.01.001

[30] Takegami K., Hayashi H., Konishi Y., et al., Development of multistage collimator for narrow beam production using filter guides of diagnostic X-ray equipment and improvement of apparatuses for practical training, Medical Imaging and Information Sciences 30, 101-107(2013). Doi: 10.11318/mii.30.101

[31] Maehata I., Hayashi H., Kimoto N. et al., Practical method for determination of air

kerma by use of an ionization chamber toward construction of a secondary X-ray field to be used in clinical examination rooms, Radiological Physics and Technology 9, 193-201(2016). Doi: 10.1007/s12194-016-0352-7

[32] Hirayama H., Namito Y., Bielajew A.F., et al., The EGS5 Code System, SLAC Report number: SLAC-R-730, KEK Report number: 2005-8. (2007).

[33] Kishida M., Hayashi H., Kuboyabu T., et al., Fabrication of a Visualization Equipment for Scattered X-rays in the Diagnosis Domain and Proposal of a Practical Training, Japanese Journal of Radiological Technology 69, 500-507(2013). Doi: 10.6009/jjrt.2013_JSRT_69.5.500

[34] Maehata I., Hayashi H., Takegami K., et al., Fabrication of Improved Multi-slit Equipment to Obtain the Input-output Characteristics of Computed Radiography Systems: Correction of the Heel Effect, and Application to High Tube-voltage Experiments, Japanese Journal of Radiological Technology 70, 867-876(2014). Doi: 10.6009/jjrt.2014_JSRT_70.9.867

[35] Kimoto N., Hayashi H., Maehata I., et al., Development of All-in-one Multi-slit Equipment for Measurements of the Input-output Characteristic of a Phosphor Plate, Japanese Journal of Radiological Technology 69, 1165-1171(2013). Doi: 10.6009/jjrt.2013_JSRT_69.10.1165

[36] Takegami K., Hayashi H., Okino H., et al., Estimation of identification limit for a small-type OSL dosimeter on the medical images by measurement of X-ray spectra, Radiological Physics and Technology 9, 286-292(2016). Doi: 10.1007/s12194-016-0362-5

Figure Captions:

Figure 1. Comparison of (a) actual testing, (b) general method and (c) proposed method for dosimetry of diagnostic X-rays. Using the proper dosimeter, we propose to perform direct measurements.

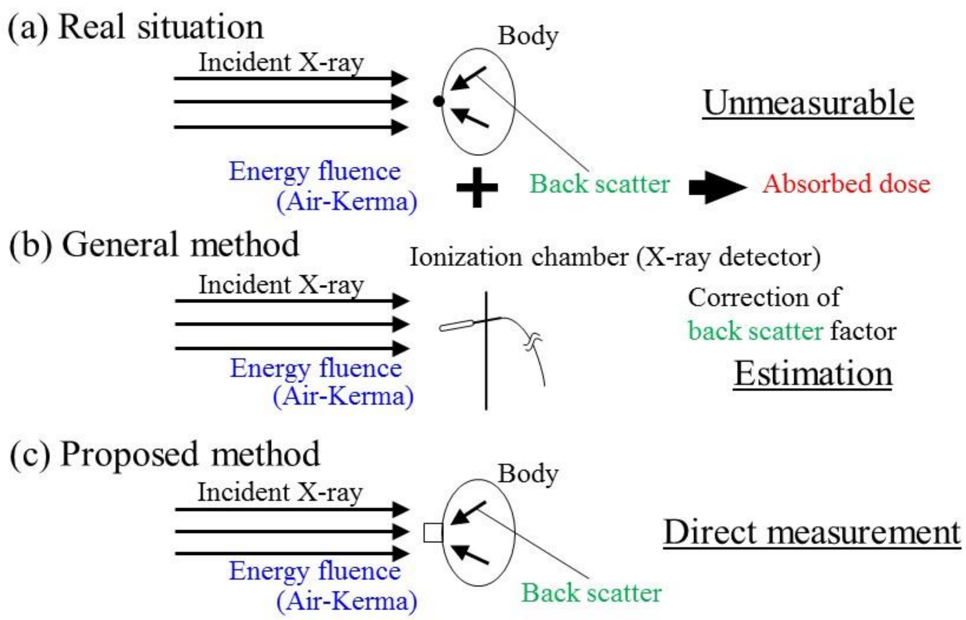

Figure 2. Detector construction of the nanoDot OSL dosimeter, which is commercially available by Landauer, Inc. The inset shows a photograph of the nanoDot OSL dosimeter.

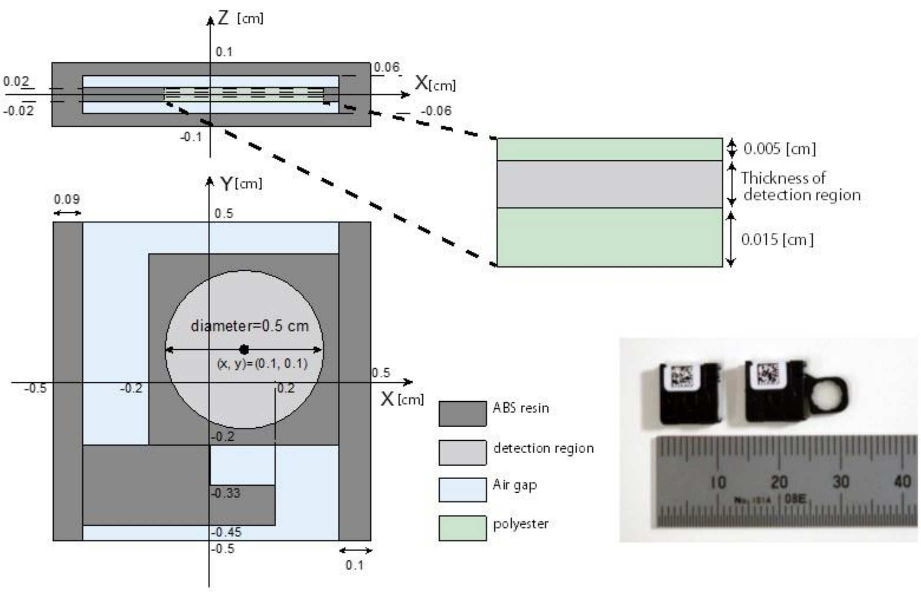

Figure 3. Schematic drawing of chest X-rays. Using the nanoDot OSL dosimeters, exposure doses corresponding to the various points can be measured.

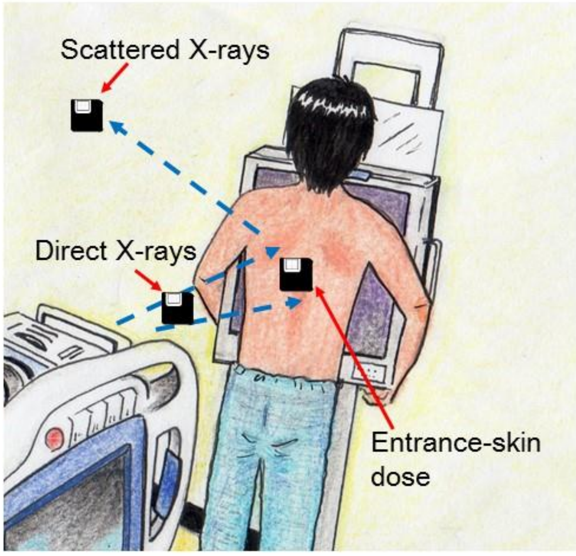

Figure 4. Demonstration of effect of AEC on the surface-dose distribution. (a) is a photograph of a phantom study. (b) and (c) show the results of surface dose distributions without and with AEC, respectively.

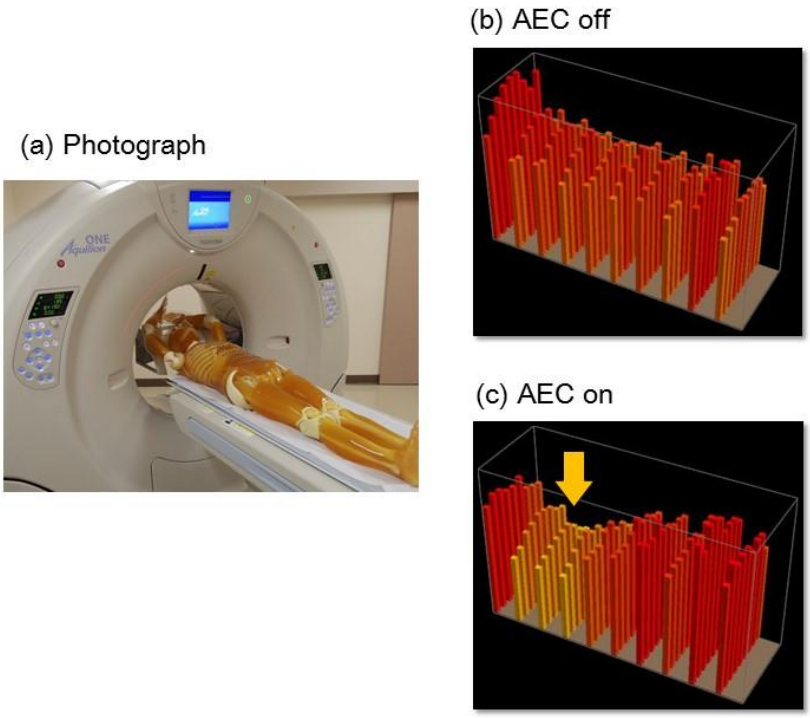

Figure 5. Angular dependence of the nanoDot OSL dosimeter. (a) is typical example for 40 kV X-rays. (b) shows change of responses when X-rays are randomly irradiated to the dosimeter.

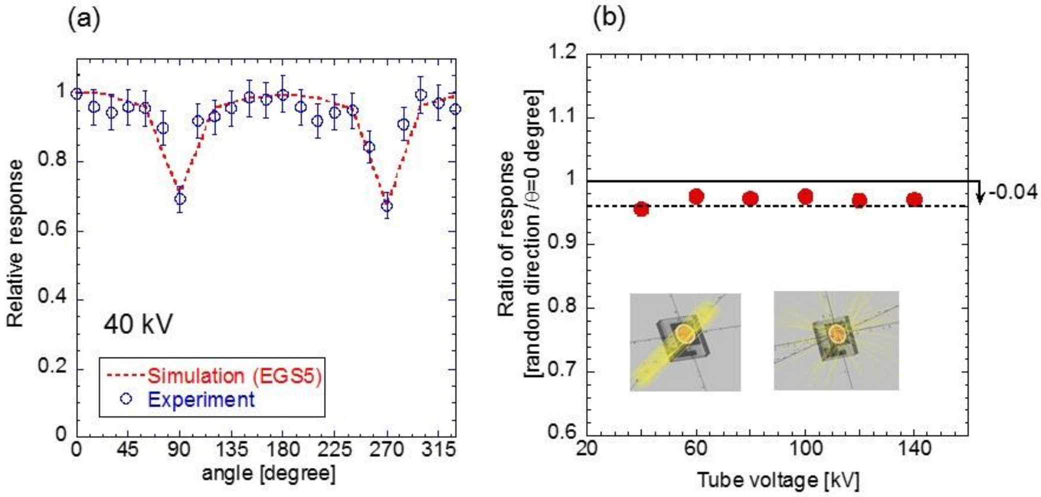

Figure 6. Energy dependence of nanoDot OSL dosimeter.

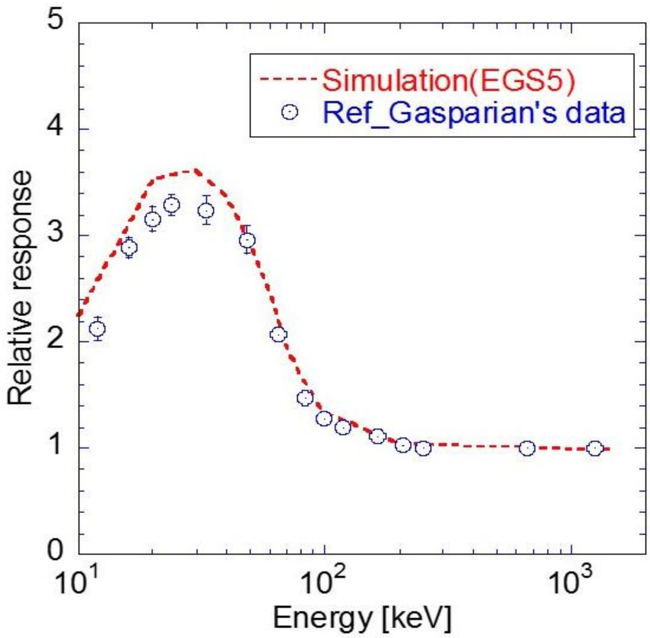

Figure 7. Proposed calibration curve for evaluating the exposure dose of nanoDot OSL dosimeter in the diagnostic energy region. The calibration curve is made from 83 kV X-rays, and we proposed that an additional 15% uncertainty should be adopted.

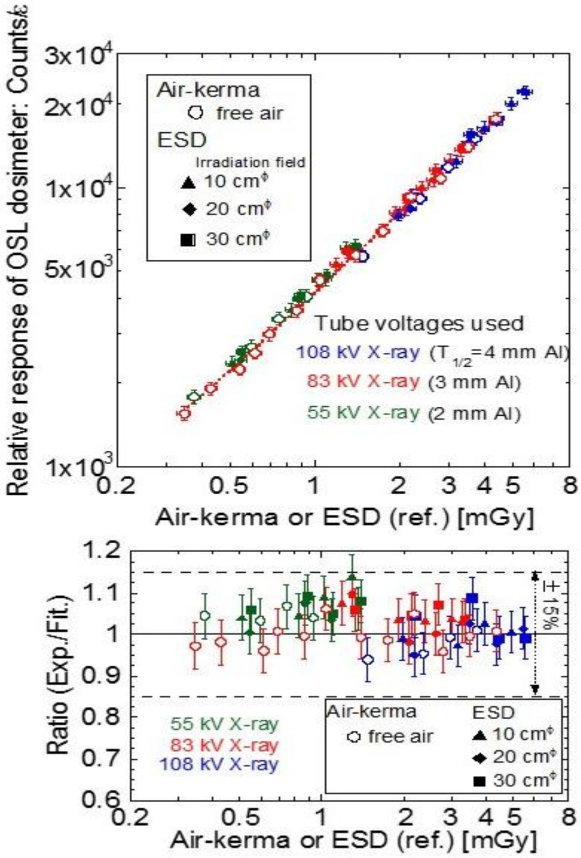

Figure 8. Typical example of direct measurement of exposure dose by means of the nanoDot OSL dosimeters. (a) shows experimental setup of the chest X-ray examination. (b) shows experimental setup of CT examination for whole body scan. (c) shows obtained X-ray image of chest X-ray, and we cannot clearly detect the nanoDot OSL dosimeters. (d) shows a cross sectional view of a CT image in the chest region; one can identify the positions where nanoDot OSL dosimeters were attached, but there are no artifacts.

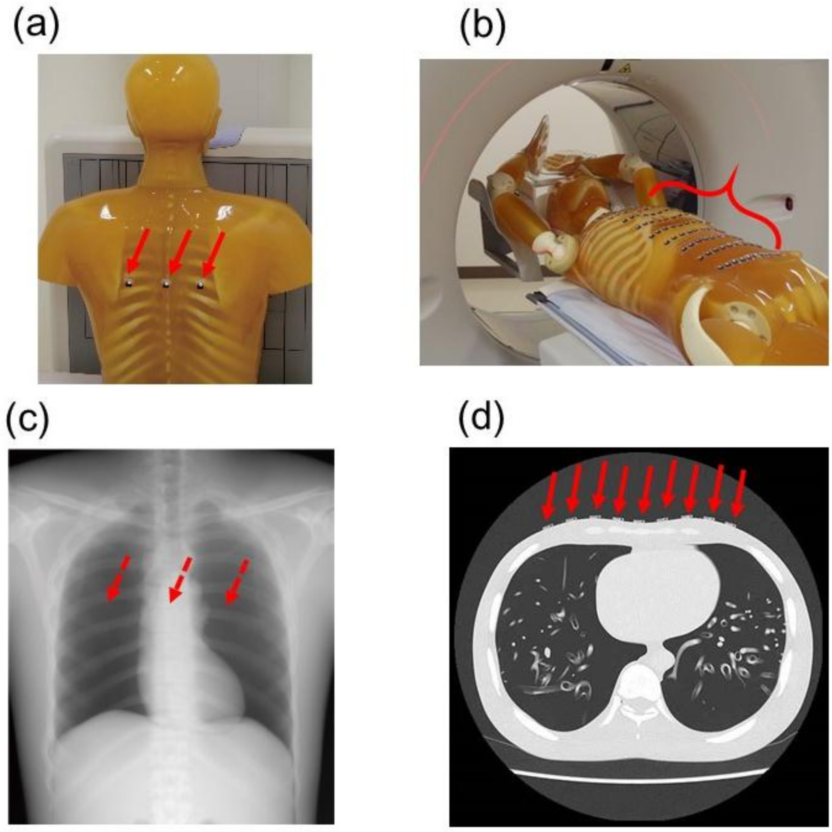

Table 1. Typically reported properties of the nanoDot OSL dosimeter.

Authors	Properties of the nanoDot OSL dosimeter		
	Composition	Thickness [mm]	Effective Density [g/cm^3]
Kerns et al. [16]	100% Al_2O_3	0.20	3.96
Lehmann et al. [17]	78.4% Al_2O_3 +21.6% Polyester	0.20	1.41
Jursinic [18]	73.1% Al_2O_3 +26.9% Polyester	0.15	2.42-2.58

